Diagnostics for the biased electrode experiment on NSTX[a)]

A. L. Roquemore,[1] S. J. Zweben,[1] R. Kaita,[1] R. J. Marsalsa,[1] C. E. Bush,[2] and R. J. Maqueda[3]
[1]*Princeton Plasma Physics Laboratory, Princeton, New Jersey 08543, USA*
[2]*Oak Ridge National Laboratory, Oak Ridge, Tennessee 37831, USA*
[3]*Nova Photonics Incorporated, Princeton, New Jersey 08540, USA*

(Presented 14 May 2008; received 12 May 2008; accepted 11 August 2008; published online 31 October 2008)

A linear array of four small biased electrodes was installed in NSTX in an attempt to control the width of the scrape-off layer by creating a strong local poloidal electric field. The set of electrodes was separated poloidally by a 1 cm gap between electrodes and were located slightly below the midplane of NSTX, 1 cm behind the rf antenna, and oriented so that each electrode is facing approximately normal to the magnetic field. Each electrode can be independently biased to ± 100 V. Present power supplies limit the current on two electrodes to 30 A and the other two to 10 A each. The effect of local biasing was measured with a set of Langmuir probes placed between the electrodes and another set extending radially outward from the electrodes, and also by the gas puff imaging diagnostic located 1 m away along the magnetic field lines intersecting the electrodes. Two fast cameras were also aimed directly at the electrode array. The hardware and controls of the biasing experiment will be presented and the initial effects on local plasma parameters will be discussed. © *2008 American Institute of Physics.* [DOI: 10.1063/1.2981166]

I. INTRODUCTION

An array of small biased electrodes were installed in the scrape-off layer (SOL) of NSTX in order to explore the theory of SOL broadening proposed by Cohen and Ryutov[1] and Ryutov *et al.*[2] by creating "toroidally asymmetric variations in the electrostatic potential." The application of this theory could mitigate the harmful effects of high peaked heat flux in the divertor of next-step machines. Biasing, as opposed to the other methods of creating toroidal variations in the potential, has the flexibility of being able to scan a range of parameters with the greatest control. It was not the intention of this experiment to make global changes in the SOL parameters but rather to design an experiment where the local effects of biasing could be accurately measured and compared to predictions. Partial confirmation of the theory has already been obtained by several experiments, most notable by an experiment on MAST where ribs on the divertor floor were alternately biased and grounded, with the result that peak heat fluxes were reduced by as much as 75% for certain cases.[3]

On NSTX, a poloidal array of four small electrodes was installed in the far-SOL near the outboard midplane to study the effects of electrostatic biasing. These effects were measured using a poloidal as well as radial array of Langmuir probes in close proximity to the electrodes. In order to measure the effects of biasing ~1 m upstream of the electrode array, the gas puff imaging (GPI) diagnostic was employed. Also, two visible cameras viewed the electrodes to look for any changes in visible light in the vicinity of the electrodes.

According to the theory, some fraction of the electrode bias should appear on the flux tubes intersecting the electrodes so a poloidal electric field, E_{pol}, will be formed between flux tubes of different potential. This electric field drives the radial convective flows, V_r, where

$$V_r = 10^8 E_{\mathrm{pol}}(\mathrm{V/cm})/B_{\|}(G).$$

Therefore, for $B_{\|}$ of ~2.5 kG in the NSTX edge, an E_{pol} of only 5 V/cm will drive V_r faster than natural turbulent transport velocities of 10^5 cm/s.[4] By biasing adjacent electrodes with opposite polarity, using the present available power supplies, a vacuum poloidal electric field of up to ~200 V/cm could be applied between the flux tubes which (if this appeared in the plasma), would create a convective flow velocity of $V_r = 5 \times 10^6$ cm/s, which should easily be large enough to affect the SOL.

The present paper details the electrode arrangement and the diagnostics required to measure the effects of electrode biasing and presents some initial data. A future paper will describe more details on the measurements.[5]

II. DESCRIPTION OF ELECTRODE/PROBE ARRAY

Figure 1 shows a layout of the four-electrode array. Each electrode is formed from 0.3 cm thick stainless sheet and has a 3×3 cm^2 square face. The electrodes were embedded into a 3 cm thick block of boron nitride (BSZN variety) to form a linear array with a 1 cm gap between adjacent electrodes. The front face of each electrode was recessed by ~1 mm into the BSZN and a small gap was made between and behind the electrode edge and the BSZN in order to reduce the possibility of electrical shorts forming between the electrodes due to plasma deposition on the front face of the insulator. This precaution of recessing the electrodes was essential since NSTX is now evaporating lithium into the plasma for density control. The leading edge of each elec-

[a)]Contributed paper, published as part of the Proceedings of the 17th Topical Conference on High-Temperature Plasma Diagnostics, Albuquerque, New Mexico, May 2008.

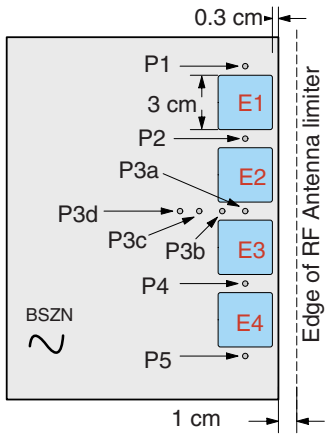

FIG. 1. (Color online) Schematic of the relative locations of the four-electrode (E1–E4) and 8 Langmuir probes (P1–P5, P3a–P3d) mounted in the BSZN substrate.

trode (the edge closest to the plasma) is only 3 mm from the leading edge of BSZN. Each electrode has a stainless screw welded into the center of the backside of the electrode for mounting and to make the electrical connection. The BSZN was chosen as the substrate material because it is an excellent electrical insulator, provides a reasonable good heat sink and has good structural integrity required to support the array ~14 cm from the vessel wall.

Also seen in Fig. 1 is a set of Langmuir probes installed in the substrate to characterize the localized effects of the electrode biasing on the plasma. Probes P1–P5 were installed on either side of the electrodes to form a poloidal array and probes P3a–P3d form a radial array with a 12.7 mm spacing between probe centers. The probes were each made from 8–32 SS threaded rod with the tips machined down to 3 mm diameter, and were threaded into the BSZN substrate from the back so that the tips were flush with the surface. A gap of ~0.5 mm was left between the edge of the probe and the BSZN, again to prevent short circuiting from plasma deposits. Channels were machined into the back of the BSZN plate (not shown) to accommodate the cables for both the electrodes and probes and a 6 mm thick plate of standard boron nitride was placed over the back side for further protection.

III. ARRAY LOCATION

The electrode array was specifically located on the magnetic field lines that pass through the region viewed by the GPI diagnostic as determined by the equilibrium code EFIT.[6] The GPI diagnostic, as described in detail in Ref. 7, utilizes a gas puff of either helium or deuterium to visibly enhance turbulence effects in the SOL. The gas puff cloud is viewed by a fast visible camera at up to 120 K frames per second to determine the space-time effects of turbulent filaments often referred to as blobs (5).

The array was secured to the vessel wall using a SS angle bracket as a support and was located 20° below the midplane to accommodate the steep pitch angle of the magnetic field lines at the edge of NSTX. The faces of the electrodes were aligned along a poloidal plane so that the electrodes were near perpendicular to the magnetic field lines.

IV. OPERATIONS OF THE ELECTRODE AND PROBE ARRAY

Each of the four electrodes has it's own dedicated, independently controlled, power supply. Each electrode can be biased to positive or negative values or grounded with respect to the vacuum vessel or it can be allowed to float. While each of the four supplies can provide 0–100 V, the two positive supplies can deliver 30 A of current while the two negative supplies are limited to 10 A. In order to clearly see the difference between the bias and no bias case, the electrode bias is typically modulated at 50 Hz. The applied voltage and the resulting current waveforms are recorded at a rate of 20 kHz for each of the electrodes.

The entire probe array is biased in unison by a single Kepco bipolar operational power supply. For measurements of temperature, the probe voltages can be swept at between ±50 V at a rate of up to 1 kHz. The probes can also be floated to measure their floating potential and can also have a fixed ± bias to measure electron or ion saturation currents to determine the local plasma density. The probe voltages and currents are acquired at a faster rate than the electrodes of 200 kHz in order to determine the effects that biasing may have on local fluctuations.

V. INITIAL RESULTS

The initial data for the biased electrode experiment presented here were obtained during Ohmic plasmas, but similar results were also obtained with neutral beam injection heated plasmas.[5]

A. *I* versus *V* curves

Figure 2(a) shows the currents drawn by the biased electrodes as a function of their voltage for a set of typical NSTX discharges with I=0.8 MA, B=4.5 kG (Nos. 123679–123684). The voltages were varied from shot to shot and the currents shown were averaged over the steady-state period from 200 to 300 ms, where the outer gap (which affects the edge plasma density) varied from ~4 to ~1 cm. The ion current was saturated for negative bias of more than −40 V, but because of initial limits on the power supplies, the positive scan was only carried out to +40 V, where the electron current is just starting to roll over due to saturation. From this plot, the measured ratio of $I_{e(\mathrm{sat})}/I_{i(\mathrm{sat})} \sim 7$, which is much higher than the expected ratio of ~1 for the "double-probe" model of electrode biasing.[2]

Figure 2(b) shows the I versus V curve obtained for probe P2 for one of these discharges. This probe has an ion saturation current of ~0.01 A or 10^{-2} that of the nearby electrode, which is consistent with the area ratio of the probe to that of the electrode. However, the ratio of electron to ion saturation current in the probe is $I_{e(\mathrm{sat})}/I_{i(\mathrm{sat})} \sim 24$, which is much higher than that for the electrodes. This may be due to a perturbing effect of the large electron current on the magnetic flux tube connected to the electrode.

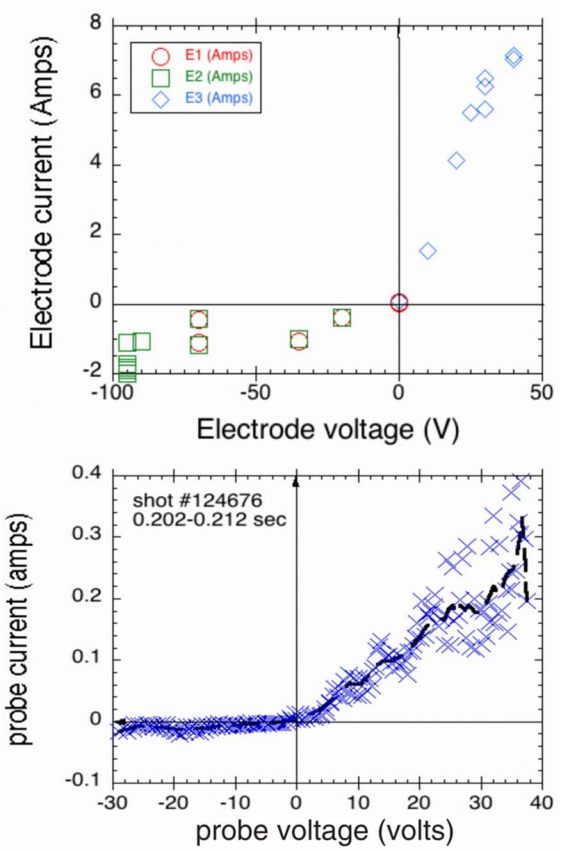

FIG. 2. (Color online) Current vs voltage curves for the biased electrodes and nearby probes. The ratio of $I_{(\mathrm{sat})e}/I_{(\mathrm{sat})i} \sim 7$ is obtained for the electrodes and $I_{(\mathrm{sat})}e/I_{(\mathrm{sat})i} \sim 24$ for the probes. The electron temperature deduced from the probe (I-V) curve was $T_e \sim 10 \pm 5$ eV.

B. SOL broadening

Evidence of SOL broadening during the electrode biasing experiment is provided by the radial probe array. Data were taken during a different set of discharges when E2 was modulated at −90 V and E3 was modulated at +90 V. The signal from the radial probe array, P3a–P3d, lying between the two electrodes was averaged over 9 cycles of the "bias on" phase and over 7 cycles for the "bias off" phase. Figure 3 shows the resulting profile changes due to biasing for Ohmic plasmas. A clear increase in probe current is observed during biasing, indicating an increase in density which is at least qualitatively consistent with movement of the SOL, as predicted in Refs. 1 and 2.

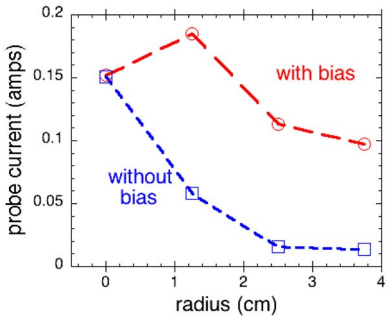

FIG. 3. (Color online) Response of the probe electron saturation current profile to electrode biasing. The probe voltages were all fixed at +45 V, while E2 was biased to −95 V, and E3 was biased to +95 V. The profiles showed an increase in SOL width during the bias on phase, implying an increase in density consistent with broadening of the SOL.

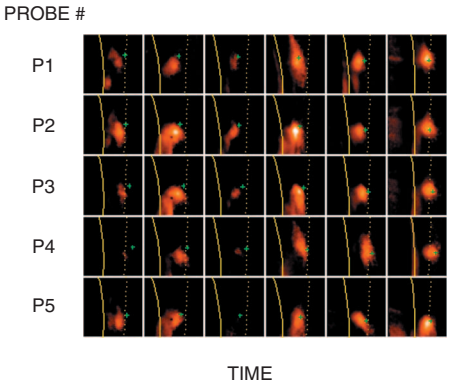

FIG. 4. (Color) Field lines incident on the probes pass through the viewing region of the GPI diagnostics resulting in areas of good correlation (white regions) between the probe signal and the D_α emission. Each square represents 24×24 cm^2 approximately with the separatrix indicated by a solid line and the antenna limiter shadow with a dotted line. The images displayed represent the correlation for a 4 ms time interval between each position in the GPI images and the probe indicated on the left. The position of the center of each probe mapped along the field line is indicated by a green plus sign.

C. Gas puff imaging

The biasing system was designed such that the magnetic field lines incident on both the electrodes and probes would pass through the viewing region of the GPI diagnostic. The exact location of the probes in the GPI field of view was determined by cross correlating the turbulent fluctuations as measured by the probes with the D_α light emission fluctuations as observed by the GPI fast visible camera. Figure 4 shows a two-dimensional radial versus poloidal mapping of the GPI field of view with red/white coloring indicating regions with a high correlation coefficient between individual probes (top to bottom) versus time (left to right), averaged over 10 ms intervals. The solid line in each frame shows the location of the separatrix. The mapping shows a high level of maximum correlation for each probe with a corresponding GPI region (≥ 0.8), indicating that they both view the same turbulent "blobs" or "filaments," which are known to have a long (>1 m) correlation length along the magnetic field. The radial and poloidal size of these regions of ~ 4 cm is the typical blob size for NSTX.[4] This is a direct confirmation that the GPI and probe diagnostics measure the same turbulent fluctuations.

If the electrode bias potentials propagated along the flux tubes to the GPI location, we would expect a change in the time-averaged D_α radial emission profile corresponding to the broadening of the SOL profile seen in Fig. 3, similar to results seen in MAST.[3] However, no consistent changes in these have been seen so far,[5] suggesting that the electrode potentials do not propagate ~ 1 m along B (although there were some subtle changes in the turbulence motion correlated with electrode biasing).

D. Fast cameras

Two cameras were used to view the electrode array itself. One camera viewed a close up of the electrodes from ~40 cm away along B, and the other camera viewed more of a global view of region around the array from across NSTX. In general, no significant changes were seen in the visible light (including D_α) during biasing. This was most likely due to the fact that the electrodes were in the "far-SOL" in the shadow of the rf antenna, and so the local light emission at the electrodes was smaller than the background of other light emission along these views. Thus these cameras were not a useful diagnostic of the local SOL effects of the biasing.

ACKNOWLEDGMENTS

The authors would like to thank Tom Holoman, Doug Labrie, Larry Guttadora, and Westly Reese for their technical expertise in the fabrication and installation of the array. This work was performed under the auspices of the U.S. Department of Energy Contract No. DE-AC02-76Ch03073.

[1] R. H. Cohen and D. D. Ryutov, Nucl. Fusion **37**, 621 (1997).
[2] D. D. Ryutov, P. Helander, and R. H. Cohen, Plasma Phys. Controlled Fusion **43**, 1399 (2001).
[3] G. Counsell, R. H. Cohen, P. Helander, and D. D. Ryutov, *Proceedings of the 30th EPS Conference on Constr. Fusion and Plasma Physics*, St. Petersburg, 7–11 July 2003, ECA, Vol. 27A, p. 3.202.
[4] S. J. Zweben, R. J. Maqueda, D. P. Stotler, A. Keesee, J. Boedo, C. E. Bush, S. M. Kaye, B. LeBlanc, J. L. Lowrance, V. J. Mastrocola *et al.*, Nucl. Fusion **44**, 134 (2004).
[5] S. J. Zweben, R. J. Maqueda, L. Roquemore, C. E. Bush, R. Kaita, R. J. Marsala, Y. Raitses, R. H. Cohen, and D. D. Ryutov, *Proceedings of the 18th Mater., International Conference on Plasma Surface Interactions* (to be published).
[6] S. A. Sabbath, S. M. Kaye, J. Menard, F. Paoletti, M. Bell, R. E. Bell, J. M. Bialek, M. Bitter, E. D. Fredrickson, D. A. Gates, A. H. Glasser *et al.*, Nucl. Fusion **41**, 1601 (2001).
[7] R. J. Maqueda, G. A. Wurden, D. P. Stotler, S. J. Zweben, B. LaBombard, J. L. Terry, J. L. Lowrance, V. J. Mastrocola, and G. F. Renda, Rev. Sci. Instrum. **74**, 2020 (2003).